The Astrophysical Journal, 585:355–371, 2003 March 1


# CHEMICAL EVOLUTION IN PROTOSTELLAR ENVELOPES: COCOON CHEMISTRY

S. D. Rodgers and S. B. Charnley
NASA Ames Research Center, Space Science Division, MS 245-3, Moffett Field, CA 94035
*Received 2002 May 15; accepted 2002 October 10*

## ABSTRACT

We have modeled the chemistry that occurs in the envelopes surrounding newborn stars as they are gradually heated by the embedded protostar and the ice mantles of dust grains evaporate, resulting in a hot molecular core. We consider two dynamical scenarios: (1) a cloud undergoing the "inside-out" gravitational collapse calculated by Shu and (2) a quasi-stationary envelope. The radial distribution of dust temperature means that differences in surface binding energies result in distinct spatial zones with specific chemistries, as more volatile species (e.g., $H_2S$) are evaporated before more tightly bound species (e.g., $H_2O$). We use our results to identify chemical features that depend on the nature of the collapse and so determine observational tests that may be able to distinguish between different dynamical models of the star formation process. We show that the observed molecular abundances in massive hot cores can be explained only if these objects are supported against collapse.

*Subject headings:* astrochemistry — ISM: abundances — ISM: clouds — molecular processes — stars: formation

## 1. INTRODUCTION

Molecular chemistry can provide insight into the physical processes in the earliest stages of starbirth, when molecular cloud cores collapse to form protostellar condensations (e.g., van Dishoeck & Blake 1998). These dense cores can be probed by observing dust emission in the far-infrared and molecular lines at millimeter and submillimeter wavelengths. In recent years, many advances in these areas have been made (see, e.g., André, Ward-Thompson, & Barsony 2000; Stahler, Palla, & Ho 2000). However, observations of dust and molecules such as CO necessarily trace the entire envelope; determining the structure of the protostellar clump on the finest scales requires observations of molecules that are present only in the very inner regions of the envelope. As newly formed stars heat the dust grains in the surrounding natal cocoon, molecular ices that have accreted onto the grains in the prestellar cold phase are evaporated. Thus, these evaporated molecules provide excellent tracers of the innermost material surrounding the protostar.

As they have intrinsically more mass, the column densities of evaporated molecules are much larger toward massive protostars than toward low-mass protostars. Such regions have been identified and studied for around two decades and are known as hot molecular cores (hereafter "hot cores"). The energy source responsible for heating hot cores has been debated over the years, but recent calculations have shown that they most likely possess an embedded source in their center (Kaufman, Hollenbach, & Tielens 1998; Osorio, Lizano, & D'Alessio 1999). Further evidence for centrally embedded protostars in hot cores comes from their centrally peaked density and temperature profiles and their association with ultracompact H II regions and maser emission (Kurtz et al. 2000). Kurtz et al. proposed that hot cores represent one of the earliest stages in the evolution of massive stars, occurring almost immediately after the protostar forms but before it is sufficiently powerful to ionize all the surrounding gas.

Observationally, hot cores are characterized by compact sources of warm, dense gas with large abundances of molecules such as $NH_3$ and $H_2O$ and anomalously large D/H ratios for their high temperature (e.g., Blake et al. 1987). It has long been known that the chemical composition of hot cores reflects the recent evaporation of interstellar grain ice mantles, and numerous models of the chemistry in these regions have been developed (e.g., Brown, Charnley, & Millar 1988; Charnley, Tielens, & Millar 1992; Charnley, 1995; Caselli, Hasegawa, & Herbst 1993). In addition to simple species like water, methanol, and ammonia, hot cores also contain many other more complex organic molecules (Ehrenfreund & Charnley 2000). Some of these molecules are thought to be "daughter" molecules, formed in situ in the hot gas from chemical reactions of the original "parent" species (e.g., Millar, Herbst, & Charnley 1991; Charnley et al. 1992, 1995). Thus, detailed chemical models are essential in order to understand the nature of the initial ice composition and to explain differences between individual hot cores and determine their evolutionary state.

High-mass protostars are capable of heating large volumes of gas, whereas in low-mass protostars, the luminosity is insufficient to heat such large amounts of gas, and only the ices in the very inner region of the envelope will be evaporated. However, van Dishoeck et al. (1995) observed the typical hot-core molecules $CH_3OH$, $CH_3CN$, and $H_2CO$ in the gas phase toward the low-mass protobinary source IRAS 16293−2422. This source is also known to possess huge HDCO and $D_2CO$ fractionations (van Dishoeck et al. 1995; Loinard et al. 2001), which can be accounted for only by recent evaporation of formaldehyde from grains (Ceccarelli et al. 2001). Ceccarelli et al. (2000) modeled the envelope of this object and concluded that the abundant $H_2O$ and SiO in the inner region must result from ice evaporation. Another low-mass protostar, Elias 29, also shows the presence of hot CO and $H_2O$ within a few hundred AU of the central object (Boogert et al. 2000). Thus, it is likely that most low-mass protostellar envelopes also harbor hot cores.

Small-scale spatial differentiation is observed in the chemical composition of many hot cores. For example, in Orion-KL the hot-core source appears to be enriched in N-bearing species, whereas the Compact Ridge has enhanced levels of O-bearing species (Blake et al. 1987). Similar spatial differentiation is seen in other hot cores, e.g., W3(OH) (Wyrowski et al. 1999), G29.96−0.02 (Pratap, Mageath, & Bergin 1999), G5.89−0.39 (Thompson & Macdonald 1999), and Sgr B2 (Nummelin et al. 2000). This effect was originally explained by different initial ice compositions (Charnley et al. 1992), due to different surface formation rates of $NH_3$ and $CH_3OH$ in distinct regions of the natal cloud (Caselli et al. 1993). However, measurements of interstellar ice compositions cast doubt on this explanation (e.g., Gibb et al. 2000b; Gibb, Whittet, & Chiar 2001), and in a recent paper we showed how such differentiation may arise as an age/temperature effect (Rodgers & Charnley 2001a, hereafter Paper I). Similar effects may be apparent in the sulfur chemistry and observations of sulfuretted molecules may be used as a "chemical clock" to determine the ages of hot cores (e.g., Charnley 1997; Hatchell et al. 1998a).

Alternatively, it is possible that spatial differentiation could arise as a result of differential evaporation of ice species with different surface binding energies (e.g., Walmsley & Schilke 1993). This idea receives some support from observations demonstrating that interstellar ices consist of both polar ($H_2O$ rich) and nonpolar (CO rich) ice phases (Ehrenfreund et al. 1998a; see Tielens et al. 1991). There is also evidence for an ice phase consisting of $CH_3OH$—$CO_2$ complexes (Dartois et al. 1999a). In this scenario, cooler hot cores would contain only the most volatile surface species, whereas in hotter regions the entire ice mantles will have evaporated. Since the inner regions of the protostellar envelope will be hotter than those further from the protostar, we may expect hot cores to display an "onion-skin" type layered structure with distance from the protostar (see Fig. 4 of van Dishoeck & Blake 1998). There is indeed observational evidence for this picture. For example, Millar, Macdonald, & Gibb (1997b) fitted observations of the hot core G43.3+0.15 with a core-halo model, and Wilson et al. (2000) derived a similar structure for the Orion hot core from ammonia mapping. Molecular surveys of hot cores also show that the higher energy transitions tend to trace more compact regions and that methanol appears to have a more extended distribution than $CH_3CN$ and other nitrile species in a variety of sources (Hatchell et al. 1998b; Gibb et al. 2000a; Dartois, Gerin, & d'Hendecourt 2000).

Van der Tak et al. (1999, 2000a, 2000b) and Lahuis & van Dishoeck (2000) have observed a number of molecules in massive protostellar envelopes, including CO, CS, $H_2CO$, $HCO^+$, $CH_3OH$, HCN, and $C_2H_2$. The observations of methanol and acetylene can only be explained if there is a discontinuous jump in the abundances when the temperature reaches ~100 K, providing direct evidence that hot cores result from mantle evaporation in the inner regions of protostellar cocoons. However, the large HCN abundances seen in the centers of these objects cannot be explained solely by evaporation of ices, and it appears that hot gas phase chemistry must be responsible (Boonman et al. 2001). This agrees with our earlier model calculations (Paper I), which show that at high temperatures HCN can be produced in copious amounts from evaporated ammonia. Thus, hot-core molecular abundances and their spatial distributions are likely to result from a combination of three factors: (1) differential evaporation of more volatile molecules in the outer regions, (2) high-temperature gas phase chemistry in the inner regions, and (3) the dynamical evolution of the cloud, which determines how long each shell of gas spends in a particular density and temperature regime. Therefore, in order to fully understand hot-core chemistry, it is necessary to calculate the chemical evolution in a physically realistic protostellar envelope that is evolving dynamically.

To date, most chemical models of hot cores have been simple calculations, where the chemical evolution is followed at a single position in the cloud with constant physical conditions. Millar et al. (1997b) modeled the hot core G34.3+0.15 with a multipoint, three-component core-halo model. However, they considered only four points within the actual hot-core region, and although the density in the outer halo was assumed to decrease with radius, they neglected any change in the physical conditions within the hot core. Numerous chemical models of the chemistry in collapsing cores have been published (e.g., Rawlings et al. 1992; Bergin & Langer 1997; El-Nawawy, Howe, & Millar 1997; Aikawa et al. 2001), but these models are appropriate only for the initial prestellar collapse phase, since they neglect the heating from the protostar and disk. Ceccarelli, Hollenbach, & Tielens (1996) developed a sophisticated model of protostellar envelopes, including energy balance, radiative transfer, and chemical reactions. However, this model was aimed principally at calculating the gas temperatures and line emission profiles and so contained only a limited chemistry focusing on the major gas coolants O, CO, and $H_2O$.

In this paper, we present models of the chemical evolution occurring in protostellar envelopes, within the "sphere of thermal influence" (Adams & Shu 1985). We employ physically realistic density and temperature profiles and dynamical evolution of the gas calculated from models of cloud collapse and protostar formation. Our principal aims are to account for the observed chemical composition in hot cores, to understand the origin of the spatial variations seen in certain hot-core molecules, and to identify chemical diagnostics of evolutionary state. In addition, we also consider how our results may be used to probe the physical structure of protostellar envelopes, in particular the nature of the collapse. To this end, we have performed calculations both with and without collapse to see whether large differences in the infall rate are reflected in similar differences in the resulting molecular distributions.

## 2. CHEMICAL MODEL

We use a multipoint model which calculates the time-dependent chemistry for 31 shells of gas, initially spaced at equal logarithmic intervals between $10^{14} \leq r \leq 10^{17}$ cm (~10–$10^4$ AU). Because the cloud is evolving dynamically, the position and size of each shell will change with time, so it is necessary to solve the chemistry in a frame of reference comoving with the gas. Hence, we calculate the Lagrangian time derivative, $Dn(\mathrm{X})/Dt$, for the number density of each species X in our model:

$$\frac{Dn(\mathrm{X})}{Dt} = \frac{\partial n(\mathrm{X})}{\partial t} + u\frac{\partial n(\mathrm{X})}{\partial r} \tag{1}$$

$$= G(\mathrm{X}) - n(\mathrm{X})\left(\frac{2u}{r} + \frac{\partial u}{\partial r}\right), \tag{2}$$

where $u$ is the velocity (note the convention that infall is represented by negative $u$), $G(\mathrm{X})$ is the net generation rate of X due to all chemical reactions and accretion/desorption processes, and we have assumed spherical symmetry.

The chemical reaction network we use is based on the UMIST RATE95 database (Millar et al. 1997a) and consists of 207 species linked by 2337 reactions. A brief overview of the additional reactions we have included is given in Paper I; a full description will appear in S. B. Charnley & S. D. Rodgers (2003, in preparation). Freezeout and desorption rates are calculated explicitly for each species (see below).

### 2.1. *Accretion*

For neutral molecules the freezeout rate, $\lambda$, is given by (e.g., Charnley, Rodgers, & Ehrenfreund 2001)

$$\lambda(\mathrm{X}) = 4.55 \times 10^{-18} \left[\frac{T}{m(\mathrm{X})}\right]^{0.5} n_{\mathrm{H}} \quad (\mathrm{s}^{-1}) \,, \tag{3}$$

where $T$ is the gas temperature, $m(\mathrm{X})$ is the molecular weight of species $X$, $n_{\mathrm{H}}$ is the total hydrogen nucleon density ($\mathrm{cm}^{-3}$), and we have assumed unit sticking efficiency, a mean grain radius of 0.1 $\mu$m, and a grain abundance of $10^{-12}$. Equation (3) applies to all neutrals except hydrogen molecules and helium atoms, which are assumed to remain in the gas phase. For most neutrals the loss of gas-phase molecules is assumed to correspond to the production of solid phase molecules. In the case of atomic H, we assume that this is immediately returned to the gas phase as $\frac{1}{2}\mathrm{H}_2$. For heavy atoms and simple radicals (OH, NH, $\mathrm{NH}_2$, CH, $\mathrm{CH}_2$, $\mathrm{CH}_3$, SH), we assume immediate hydrogenation on the surface.

At the densities of interest, almost all the grains will be negatively charged (Umebayashi & Nakano 1990), and so ions will collide with grains more rapidly than their neutral counterparts. For singly ionized species, the collision rate is enhanced by a factor $(1 + e/akT)$, where $e$ is the electron charge, $a$ is the grain radius, and $k$ is the Boltzmann constant. We assume that the ions are immediately neutralized on contact with the grains and undergo dissociative recombination, with the products ejected back into the gas phase (Aikawa, Herbst, & Dzegilenko 1999). Where an ion has more than one possible set of dissociation products, we assume that the branching ratios for each channel are the same as for gas-phase recombination reactions.

### 2.2. *Desorption*

The thermal desorption rate, $\xi$, of ice molecules is given by

$$\xi(\mathrm{X}) = \nu(\mathrm{X}) \exp\left\{-\frac{E_b(\mathrm{X})}{kT_d}\right\} \tag{4}$$

(Watson & Salpeter 1972), where $\nu(\mathrm{X})$ is the vibrational frequency of X in its binding site, $E_b(\mathrm{X})$ is the binding energy, and $T_d$ is the grain temperature. For all species, we assume $\nu = 2 \times 10^{12}$ $\mathrm{s}^{-1}$ (e.g., Sandford & Allamandola 1993). Values of $E_b$ are taken from the table compiled by Aikawa et al. (1997); if a neutral molecule in our scheme is not on this list we assume a default value for $E_b/k$ of 4820 K, which is equivalent to assuming that the desorption is controlled by that of $\mathrm{H}_2\mathrm{O}$.

We also consider nonthermal desorption of the most volatile molecules—CO, $\mathrm{N}_2$, $\mathrm{O}_2$, and $\mathrm{CH}_4$—based on the fact that thermal desorption is insufficient to sustain the observed abundances of gas-phase molecules in cold gas at 10 K (Charnley et al. 2001). A variety of possible mechanisms have been suggested to account for this desorption (see, e.g., Willacy & Millar 1998; Markwick, Millar, & Charnley 2000), and due to the uncertainty surrounding the nature of this process, we choose to take a pragmatic approach and simply set the nonthermal desorption rate, $\xi^{\mathrm{NT}}$, as a parameter of our model. Since $\xi^{\mathrm{NT}}$ is not a particularly important parameter (see § 4) and is in any case an estimate, we assume the same value of $\xi^{\mathrm{NT}}$ for each of the four species that are subject to nonthermal desorption. Observations of CO in dark clouds show evidence for depletion only at densities above $\sim 10^5$ $\mathrm{cm}^{-3}$ (Caselli et al. 1999), so we select a value which keeps 90% of the total CO in the gas phase for $n = 5 \times 10^5$ $\mathrm{cm}^{-3}$ and $T = 10$ K. Hence, we set $\xi^{\mathrm{NT}}$ to be 9 times the CO accretion rate under these conditions, i.e., $\xi^{\mathrm{NT}} = 1.22 \times 10^{-11}$ $\mathrm{s}^{-1}$.

### 2.3. *Initial Conditions*

We assume complete depletion of metals, and the initial chemical conditions are summarized in Table 1. Essentially, we assume that $\mathrm{H}_2\mathrm{O}$, $\mathrm{CH}_3\mathrm{OH}$, $\mathrm{H}_2\mathrm{CO}$, and $\mathrm{H}_2\mathrm{S}$ are frozen onto grains and that CO and $\mathrm{N}_2$ are partitioned between the gas and ice according to the ratio of the rates for accretion versus nonthermal desorption. Because the former increases with density, whereas the latter is assumed to be constant, the fraction of CO and $\mathrm{N}_2$ initially in the gas will decrease toward the center of the cloud. Methanol ice abundances of 30% relative to $\mathrm{H}_2\mathrm{O}$ have been observed toward the high-mass protostar RAFGL 7009S (Dartois et al. 1999b), so our $\mathrm{CH}_3\mathrm{OH}$ abundance may be an underestimate. Our assumed value is in line with the typical upper limits derived by Dartois et al. toward a number of other sources. We also assume that no ammonia is present in the initial ice composition, based on recent work that suggests that in most sources it has an abundance of less than 5% (Dartois & d'Hendecourt 2001; Gibb et al. 2001). However, we find that ion-molecule chemistry prior to infall can lead to ammonia ice abundances of $\sim$1% at the time that the infall begins and the protostar "switches on" (see below).

TABLE 1

Initial Molecular Abundances, Relative to $\mathrm{H}_2$

| Species | Phase | Abundance |
|---|---|---|
| H | Gas | 1 $\mathrm{cm}^{-3}$[a] |
| He | Gas | 0.15 |
| CO | Both[b] | 1(−4) |
| $\mathrm{N}_2$ | Both[b] | 2(−5) |
| $\mathrm{H}_2\mathrm{O}$ | Ice | 4(−5) |
| $\mathrm{CH}_3\mathrm{OH}$ | Ice | 1(−6) |
| $\mathrm{H}_2\mathrm{CO}$ | Ice | 4(−7) |
| $\mathrm{H}_2\mathrm{S}$ | Ice | 2(−7) |

Note.—The term $x(-y)$ is shorthand for $x \times 10^{-y}$.

[a] Atomic H is assumed to have a number density of 1 $\mathrm{cm}^{-3}$; hence its abundance relative to $\mathrm{H}_2$ depends on its density.

[b] The initial gas-solid ratios for CO and $\mathrm{N}_2$ are calculated according to the ratio of their accretion and (nonthermal) desorption rates.

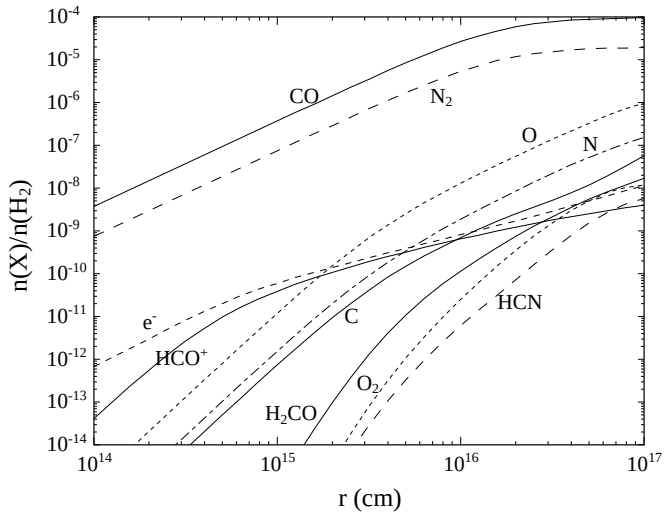


FIG. 1.—Initial quasi–steady-state molecular abundances prior to collapse, found by evolving the chemistry for $10^5$ yr in a static 10 K cloud with a density profile given by eq. (5).

At each initial position we run the chemical model for $10^5$ yr with no infall and a constant temperature of 10 K, in order to calculate the quasi–steady-state abundances of minor species, which are formed via reactions initiated by $He^+$ ions attacking the CO and $N_2$ in the gas phase. Thus, we implicitly assume that the timescale for the formation of the initial isothermal core is longer than the chemical timescale. This will be the case if the cloud is supported by magnetic fields and collapses gradually via ambipolar diffusion (Mouschovias 1978). Figure 1 shows the abundances after $10^5$ yr, just before the collapse is initiated. It is clear that as CO and $N_2$ become progressively more depleted in the inner region, the gas-phase abundances of molecules formed from them also decline. We find that this ion-molecule chemistry in the preprotostellar phase is an efficient source of ammonia ice, as a small fraction of the gas-phase $N_2$ is eroded into N and $N^+$ by $He^+$ attack. The $N^+$ subsequently undergoes successive reactions with $H_2$, leading eventually to $NH_4^+$, which recombines to give $NH_3$ and $NH_2$. These species then freeze out, and we find that after $10^5$ yr the resulting surface abundance of ammonia is $\sim$1% relative to water. Thus, even though we assume that no $NH_3$ is present in the original ice, by the time the collapse is initiated, some ammonia is present on the grains (see also Charnley & Rodgers 2002).

## 3. PHYSICAL CONDITIONS AND CLOUD DYNAMICS

In order to solve equation (2) for each species, it is necessary to know the velocity and temperature profiles at all times. As these will depend on the chemical state of the gas, a fully accurate model should calculate $u(r, t)$ and $T(r, t)$ explicitly, considering the coupling between the chemistry and the dynamics. This is important since the gas cooling rate depends on the molecular abundances, and it is this cooling that permits the cloud to dissipate the thermal energy, which supports it against further collapse. However, such a calculation is extremely computationally intensive, as it involves linking the physics and the chemistry simultaneously with the radiative transfer. The most ambitious attempt to date has been the work of Ceccarelli et al. (1996), who explicitly calculated the chemistry, gas temperature, and rotational level populations of CO and $H_2O$, but who adopted the velocity profile calculated by Shu (1977) and the dust temperature profile of Adams & Shu (1985).

As we are concerned mainly in this paper with the chemistry in the collapsing envelope, as a first approximation we simply take the results of previous dynamical models and neglect the interaction between the chemistry and the physics. With this assumption, the values of $T(r, t)$ and $u(r, t)$ are calculated a priori and are simply input into equation (2) as parameters of our model. A number of well-defined collapse models have been developed, for example, free fall (Spitzer 1978), Larson-Penston (Larson 1969; Penston 1969), and the "inside-out" collapse of singular isothermal spheres (Shu 1977) and singular logatropic spheres (McLaughlin & Pudritz 1997). We have chosen to use the results of Shu (1977), primarily because we also need to know the temperature profile and the best analytic approximations of the dust temperatures around protostars were performed by Adams & Shu (1985) for an envelope undergoing an "inside-out" collapse.

### 3.1. *Gravitational Collapse Model*

The only external parameter that affects the nature of the collapse is the sound speed, $a$, which determines the initial hydrostatic density distribution

$$\rho_0(r) = \frac{a^2}{2\pi G r^2} \tag{5}$$

and the mass accretion rate of the protostar

$$\dot{M} = 0.975 \frac{a^3}{G} , \tag{6}$$

where $G$ is the gravitational constant. The initial $H_2$ number density at each radius is calculated from equation (5) assuming a $He/H_2$ abundance of 0.15, i.e., a mean molecular mass of 2.6 amu per $H_2$ molecule. We assume a value for $a$ of 0.35 km $s^{-1}$, which yields a mass accretion rate of $10^{-5}\ M_\odot\ yr^{-1}$. This value of $a$ is almost twice the value of 0.19 km $s^{-1}$ appropriate for purely thermal cloud support at 10 K, but will be appropriate if the core is supported by additional nonthermal mechanisms such as turbulence and/or magnetic fields (Stahler, Shu, & Taam 1980). The singular isothermal sphere described by equation (5) is unstable, and Shu (1977) derived a numerical solution for its collapse following a small perturbation at the center; essentially a collapse wave propagates outward with speed $a$, and the density and velocity profiles of the infalling material asymptotically approach those for gas undergoing gravitational free fall ($n \propto r^{-1.5}$, $u \propto r^{-0.5}$). The collapse has the property of self-similarity, and one can calculate the properties in terms of the dimensionless distance variable $x \equiv r/at$.

Shu (1977) tabulated numerical values for the velocity profile in the collapsing envelope, and we use cubic spline interpolation of his results to obtain $u$ and $du/dr$ at arbitrary values of $r$. Using these values in equation (2) allows us to calculate the factor by which each fluid element is compressed as it falls in and, hence, to solve the Lagrangian time derivatives for the chemical evolution. Figure 2 illustrates the resulting $H_2$ number density profiles; the slight kinks in the curves (at $x = 0.05$) occur where the collapse becomes free fall ($u = -1.4ax^{-0.5}$), and we cease to calculate the density change from interpolation.

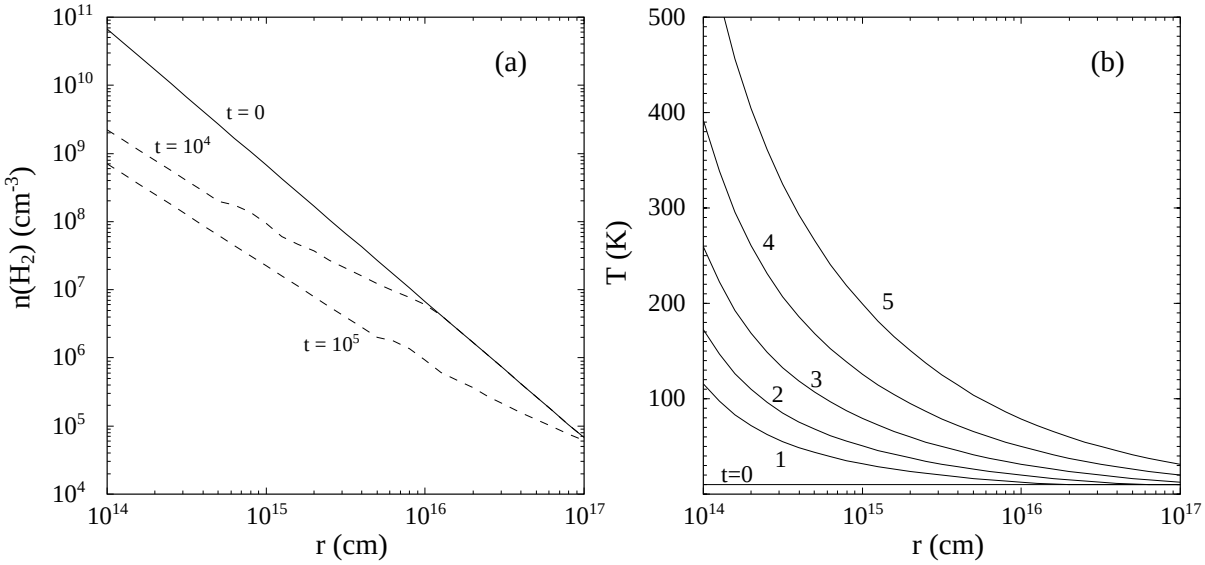


FIG. 2.—(*a*) Number density profiles for collapsing protostellar envelopes, calculated from the results of Shu (1977). (*b*) Temperature profiles in the envelope: labels give the log of the time in years. Calculated from the results of Adams & Shu (1985). In both cases the results are appropriate for a mass accretion rate of $10^{-5}\ M_{\odot}\ \mathrm{yr}^{-1}$.

The dust temperature profiles in the infalling envelope were calculated by Adams & Shu (1985) for a variety of protostellar masses and collapse rates and can be parameterized in the form

$$T_d^4(r) = [\beta_1 T_1(r)]^4 + [\beta_2 T_2(r)]^4 , \quad (7)$$

where $\beta_1$ and $\beta_2$ are dimensionless parameters and $T_1$ and $T_2$ represent the contribution from the optically thick and thin inner and outer regions, respectively. For $\dot{M} = 10^{-5}\ M_{\odot}\ \mathrm{yr}^{-1}$, Adams & Shu derived $\beta_1 = 0.62$ and $\beta_2 \approx 1.5$, and from their equation (21) it is possible to calculate $T_1$ and $T_2$ from the following expressions:

$$T_1(r) = 444.1 a^{13/6} t^{1/6} r^{-5/6} , \quad (8)$$

$$T_2(r) = 11.95 a t^{1/5} r^{-2/5} , \quad (9)$$

where $a$, $t$, and $r$ are in cgs units. The resulting temperature profiles for $a = 3.5 \times 10^4\ \mathrm{cm\ s}^{-1}$ are displayed in Figure 2. We assume that the gas temperature is equal to the dust temperature, which is a reasonable assumption given the densities in the cloud. Explicit calculations of the gas and dust temperatures in centrally condensed cores with internal heat sources show that they are very tightly coupled within $10^{17}$ cm (Ceccarelli et al. 1996; Doty & Neufeld 1997). Additionally, the density and temperature profiles shown in Figure 2 are in good qualitative agreement with the parameters derived observationally by van der Tak et al. (2000a) and Hatchell et al. (2000).

### 3.2. *Quasi-Static Cores*

In reality, as the gas in the inner envelope is heated its pressure will rise and so the infall rate will be reduced. Additional support against collapse will be provided by stellar winds and outflows (Richer et al. 2000) and by radiation pressure on the dust grains in the envelope (Kahn 1974). Thus, it is likely that the envelope will not collapse as quickly as we calculate and may in fact remain relatively stable over fairly long timescales. This will have important consequences for the chemistry, since the hot gas in the inner regions can undergo high-temperature chemical processing for a much longer period than would occur for a collapsing envelope. In order to investigate the effects of this, we repeated our calculations without collapse but kept all other aspects of the model the same.

This is also not entirely physically realistic, since the ultimate source of the protostellar luminosity that heats the gas is the kinetic energy of the infalling material. Hence, no infall implies zero luminosity, and so no support for the surrounding cloud. Numerical models of the star formation process show that $\dot{M}$ is variable, with brief bursts of rapid infall leading to luminosity increases that eventually halt the collapse; the resulting drop in $L$ allows the collapse to accelerate again, and the cycle continues (Yorke & Krügel 1977). However, once the protostar has accreted sufficient mass, nuclear burning becomes the dominant power source and cutting off the accretion will not affect the luminosity. Therefore, our static model will be most appropriate for hot cores around massive stars, since only when the mass $\gtrsim 8\ M_{\odot}$ does the intrinsic luminosity exceed the accretion luminosity (Stahler et al. 2000).

### 3.3. *Other Physical Parameters*

We assume a constant visual extinction of 10 mag. Although the actual value will vary with depth into the cloud and will be much greater than this in the inner regions, a value of 10 is sufficient to ensure that photoprocesses are effectively irrelevant. For some species, principally atoms and simple radicals and ions, the abundances will peak in the outer "skin" of the core where the extinction is $\lesssim 3$ mag (Rodgers & Millar 1996). Thus, observations of species such as $C_2H$ toward hot cores may not in fact be tracing the material in the actual hot core. However, for prototypical hot-core molecules such as $H_2O$, $NH_3$, $CH_3OH$, nitriles, large organics, and so on, the skin abundances are greatly

reduced, so we can be certain that the observed abundances represent those in the hot core. We use a cosmic-ray ionization rate of $1.3 \times 10^{-17}$ s$^{-1}$ but neglect cosmic-ray–induced photoprocesses. The initial temperature is assumed to be 10 K throughout the cloud.

## 4. RESULTS

### 4.1. *Collapse Model*

Figures 3 and 4 show the distributions of important molecules after times of $10^4$ and $10^5$ yr, respectively. From the figures it is apparent that, as expected, a sublimation front proceeds outward from the protostar, removing molecules from grain mantles. The radius of the sublimation front varies for different molecules and depends on the surface binding energy; more volatile species will leave the grains at lower temperatures than more tightly bound species and so are released into the gas phase at larger distances. In particular, the low binding energies of $H_2CO$ and $H_2S$ (1760 and 1800 K) relative to $CH_3OH$ and $H_2O$ (4240 and 4820 K) ensure that $H_2CO$ and $H_2S$ molecules are liberated from grain mantles at much larger distances than the bulk of the ices.

As a rough guide to when a molecule will be evaporated, we can use equation (4) to calculate the critical temperature, $T_{\rm crit}$, at which the desorption timescale equals 1 yr. It is easy to show that $T_{\rm crit} \approx T_b/47$, where $T_b = E_b/k$. Thus, $H_2S$ will sublimate at a temperature of $\approx$40 K, whereas ammonia and water require temperatures of 65 and 100 K, respectively. In the outer regions of the envelope where the sublimation fronts are located, the material is optically thin in the infrared, and the dust temperature is determined mainly by the term $T_2$ in equation (9). Hence, $T_d \approx 18at^{0.2}r^{-0.4}$. Rearranging this expression, one finds that the distance, $r_{\rm crit}$, of the sublimation front for a molecule that sublimates at temperature $T_{\rm crit}$ is given by

$$r_{\rm crit} \quad ({\rm cm}) \approx 1.8 \times 10^{13} \left(\frac{T_{\rm crit}}{100\ {\rm K}}\right)^{-2.5} \left(\frac{t}{\rm yr}\right)^{0.5} . \quad (10)$$

Therefore, at any particular time the $H_2S$ sublimation front will be 10 times farther from the star than the $H_2O$ sublimation front. For a singular isothermal sphere the mass enclosed within a radius $r$ is proportional to $r$. Thus, the "$H_2S$ hot core" will contain 10 times more material than the "$H_2O$ hot core" and will be typified by solid $H_2O$ and

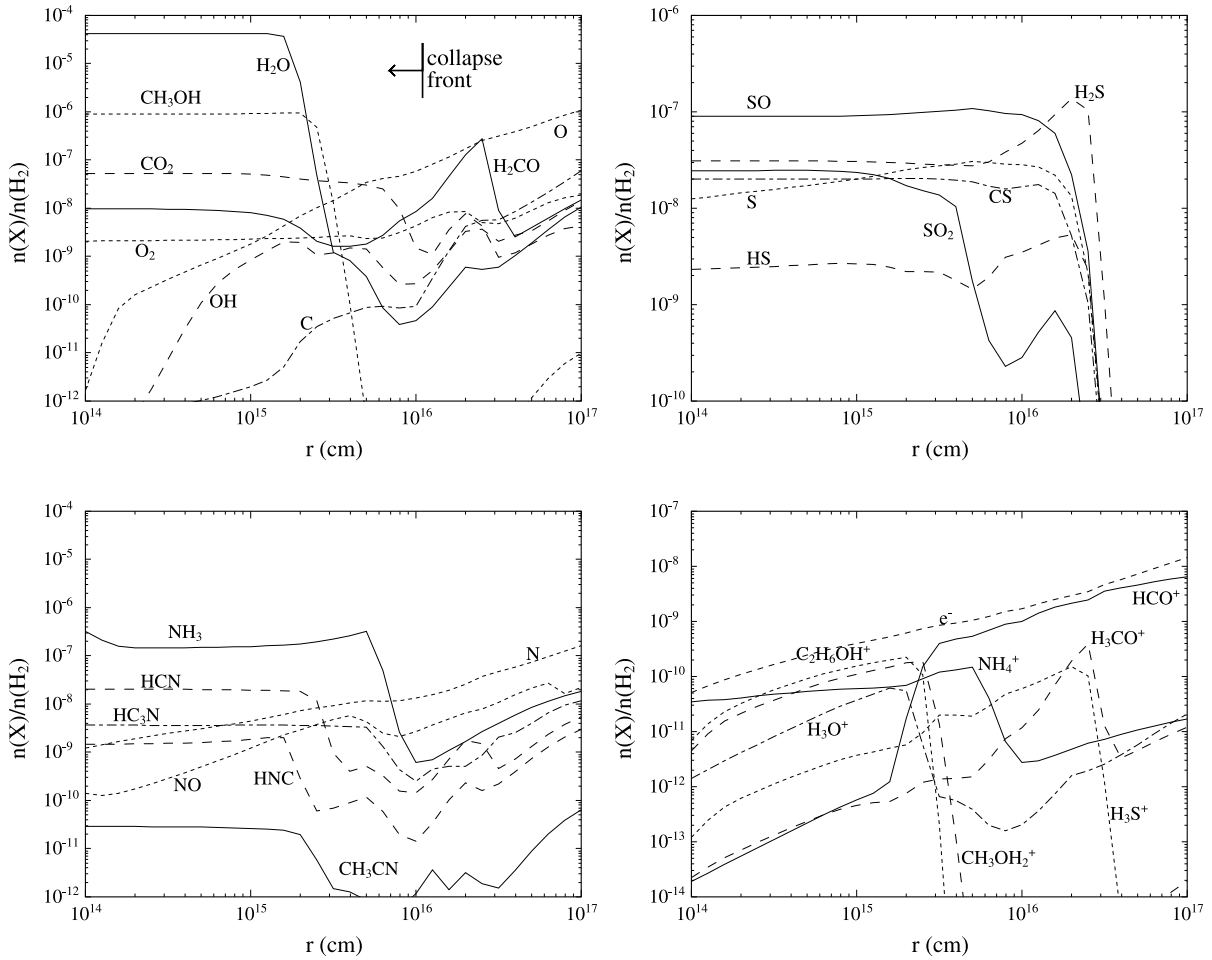


FIG. 3.—Molecular abundances in a collapsing protostellar envelope, $10^4$ yr after the collapse is initiated. Note that the $y$-axes have different scales. Also shown in the top left-hand panel is the location of the collapse front; material outside this distance is still in its original location, whereas the material inside is falling into the center.

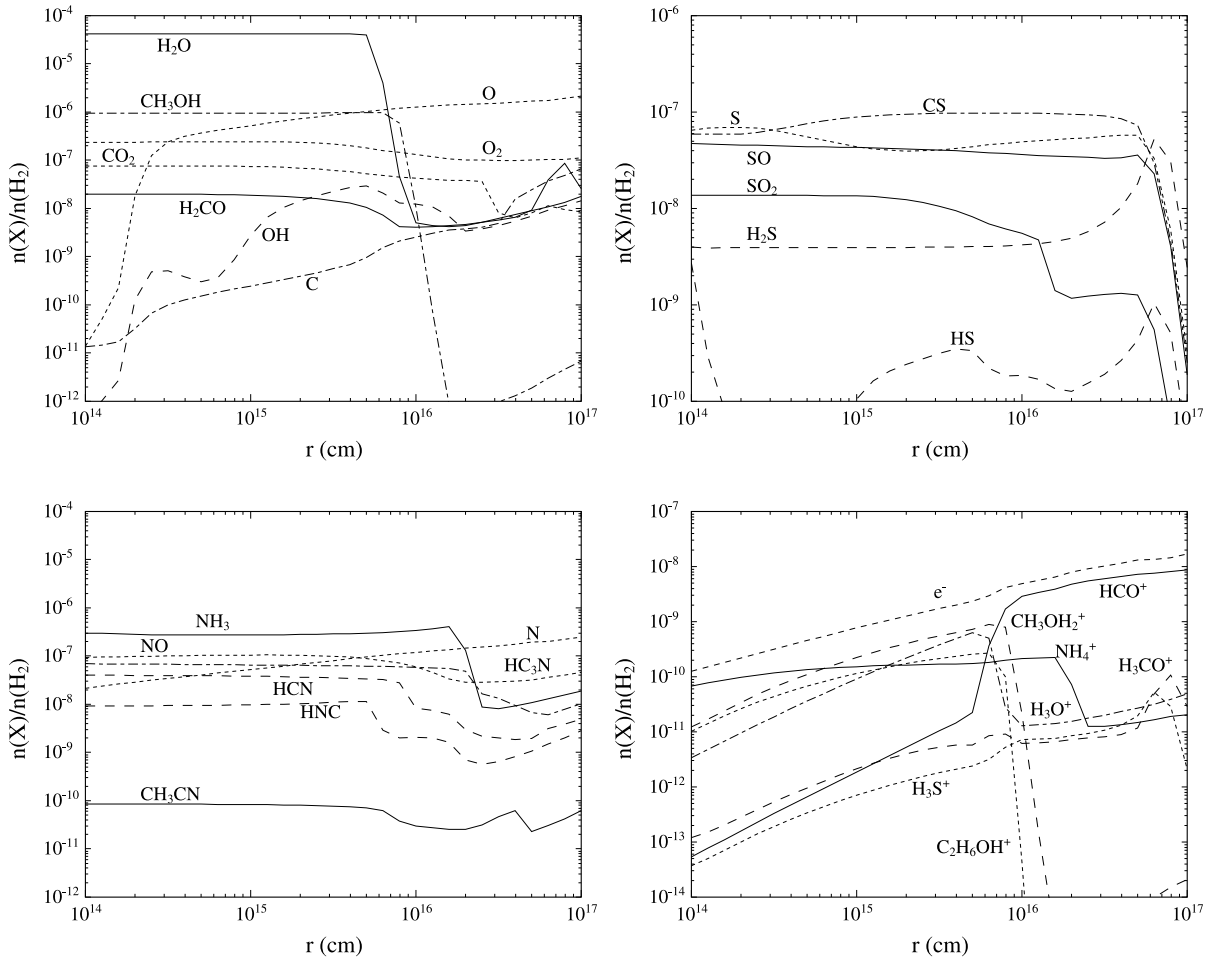


FIG. 4.—As Fig. 3, but $t = 10^5$ yr

$CH_3OH$ coexisting with gas-phase $H_2S$. Within this region a limited chemistry can occur, as $H_2CO$ and CO provide a source of gas-phase carbon and oxygen, and the parent species $H_2S$ is processed into daughter molecules such as CS, SO, and $SO_2$ (e.g., Charnley 1997).

The extreme volatility of CO means that it has a critical temperature of only 20 K, so it is rapidly returned to the gas phase after the protostar begins to heat up its envelope. For example, the gas at $r = 10^{16}$ cm reaches 20 K after only 100 yr. Since nonthermal desorption keeps most of the CO in the gas phase for $r \gtrsim 10^{16}$ cm, even at 10 K (see Fig. 1), significant amounts of solid CO should be detectable only in the youngest protostellar cores, as observed (Boogert et al. 2000). As discussed in § 2.2, the volatility of CO also implies that the uncertainty surrounding the nonthermal desorption rate, $\xi^{NT}$, will not have serious consequences for our model results, since this mechanism is rapidly overtaken by thermal evaporation.

Figures 3 and 4 show that, as demonstrated by previous hot-core models, postevaporation chemistry can transform some fraction of the parent molecules into a wide variety of daughter molecules. Protonation of $H_2O$ followed by dissociative recombination yields OH, which can then react with CO to form $CO_2$. Protonation of $CH_3OH$ leads to the $CH_3OH_2^+$ ion, which is known to undergo alkyl cation transfer reactions with many species. Evaporated ammonia will react with $C^+$ to form $HCNH^+$ (Talbi & Herbst 1998), which recombines to give HCN, HNC, and CN. These species can undergo further reactions to form $HC_3N$ and $CH_3CN$ (Paper I).

The evaporated formaldehyde has a short lifetime, which means that the $H_2CO$ abundance peaks just behind its sublimation front. This is due to two principal factors. First, when $H_2CO$ evaporates it has the largest proton affinity of the major gas-phase species, and thus it becomes the "end of the line" for the proton cascade that determines the ionization state in hot cores (see Paper I). Because ammonia, water, and methanol are still frozen, $H_3CO^+$ is removed by dissociative recombination rather than proton transfer, and two-thirds of such reactions lead to products other than $H_2CO$. In models where all parent species evaporate simultaneously, such effects are not apparent, since most molecular ions are removed via proton transfer reactions, which will always reform the original parent species. Second, we have assumed complete depletion of metals. This has a major effect on the ionization state of the hot core, as models that include metal ions tend to have slightly larger total ionization levels but much lower abundances of molecular ions (e.g., Charnley 1997). Since it is the latter reactions that eventually destroy parent species in hot cores, the absence of metals leads to shorter lifetimes for the evaporated molecules.

The other principal feature of Figures 3 and 4 that is immediately obvious is the flatness of many of the abundance curves at small radii. This is because as the material is collapsing its velocity is increasing. Hence, at some point the dynamical timescale becomes shorter than the chemical timescale, and so the gas is swept into the central protostar (and disk) before it can undergo further chemical evolution. The abundances set in the outer envelope are "frozen" into the gas as it passes rapidly through the inner region. A related effect occurs in the spherical outflows of comets and red giant stars (e.g., Rodgers & Charnley 2001b). Similar effects must be evident to some degree in all models of gravitationally collapsing clouds. As the velocity increases most rapidly in the latter stages of the collapse, a point is reached at which the infall timescale becomes less than the chemical timescale. The inside-out collapse model results in spatial chemical homogeneity in the inner core. Conversely, in other gravitational collapse models (such as the Larson-Penston one) this does not occur since nearby shells become closer with time.

The only species for which the abundance profiles in the inner envelope are not flat are ions, or those species that undergo reactions with $H_2$ that have activation energy barriers of $\sim$1000 K. In the outer regions $HCO^+$ accounts for the bulk of the ionization, with a contribution from $H_3S^+$ and $H_3CO^+$ in the region where $H_2S$ and $H_2CO$ are evaporated, whereas $CH_3OH_2^+$ and $NH_4^+$ dominate in the inner region. In addition, self-alkylation of methanol by $CH_3OH_2^+$ leads to large abundances of $(CH_3)_2OH^+$ in the inner region, and recombination of this ion leads to large abundances of dimethyl ether. However, the overall abundance of $(CH_3)_2O$ in the inner envelope is $\sim 10^{-8}$, an order of magnitude less than can potentially be achieved if the chemistry has $\sim 10^4$ yr to evolve (Paper I).

We should also stress here that, strictly speaking, our model applies only to low-mass hot cores. The total amount of mass enclosed within our outer boundary of $10^{17}$ cm is only 1.8 $M_\odot$, and after $10^5$ yr less than half of this mass is in the central star. Therefore, it may appear to be totally unrealistic to apply our model to high-mass hot cores. However, the temperature and density profiles in massive protostellar cores are known to be centrally peaked. Hence, although the physical parameters of our model will not be appropriate for high-mass cores, the qualitative agreement should be reasonably good. In particular, the decline in temperature with radius will result in different sublimation fronts for species with different binding energies, and whether or not the gas is infalling will have the same implications regarding the chemistry.

### 4.2. *Static Model*

Because the inner regions of the collapsing core are falling more quickly than they can be altered chemically, we find that Shu's collapse model cannot generate significant small-scale structure due to high-temperature chemistry in the inner core. In order to explore this issue, we have computed the chemical evolution in a static core. This model therefore resembles the multipoint model of Millar et al. (1997b), with the crucial difference that we still calculate the temperature from equation (7) and so consider the gradual heating of the gas (e.g., Viti & Williams 1999). Hence, this model also displays sublimation fronts moving out from the protostar and an onion-skin distribution of parent molecules. Whereas in the collapse model all the gas initially within $10^{15}$ cm has fallen onto the star within 2000 yr, in this model it remains in place and can undergo high-temperature chemical processing for a significant fraction of the lifetime of the hot core ($\sim 10^5$ yr).

Figures 5 and 6 show the abundance profiles in the static model at $10^4$ and $10^5$ yr. Comparison with Figures 3 and 4 shows that the chemistry is substantially different in the inner regions of a static core as compared with a collapsing core. In particular, many species that have flat abundance profiles in the collapse model (e.g., $CO_2$, $H_2CO$, HNC, $CH_3CN$, CS, SO, $SO_2$) exhibit strong radial abundance variations in the static model. The results shown in Figures 5 and 6 confirm that in order for small-scale spatial differentiation to arise in hot cores, the gas cannot be rapidly falling into the central star. Since the only difference between the two models is the collapse, the only differences will be in those regions that are undergoing infall. Thus, the outer portion of the envelope in the collapse model that is beyond the collapse wave front (i.e., $r > at$) should be chemically identical to the static model. This can be verified by comparing the abundance profiles in Figures 3 and 5 beyond $10^{16}$ cm.

The longer time spent by the gas at high temperatures leads to higher abundances of daughter species. For example, in the collapse model the maximum amount of HCN that can be formed is a few times $10^{-8}$ relative to $H_2$, or $\sim$10% of the evaporated $NH_3$. In the static model, HCN abundances of $10^{-7}$ are possible, and even more may be formed if ammonia is present in larger abundances in the initial ices (e.g., Paper I). HCN abundances of $10^{-6}$ have been observed toward a number of protostellar sources and have been attributed to high-temperature chemical synthesis (Lahuis & van Dishoeck 2000; Boonman et al. 2001). In order to test this, we ran our model with an initial $NH_3$ ice abundance of $5 \times 10^{-6}$. We found that, in the collapse model, we produce a maximum HCN abundance of $10^{-7}$, but in the static model the observed abundances of $10^{-6}$ are easily achieved. Thus, if the HCN observed toward protostars is indeed a result of high-temperature chemistry, this has two implications for these sources. First, it implies that ammonia must be present in the evaporated ices with an abundance relative to water of $\sim$10% (note that even with no initial $NH_3$ the observed HCN abundances can eventually be attained, but only after $\sim 10^6$ yr—such ages seem unlikely for massive hot cores). Second, it implies the gas in which the HCN is situated is supported against collapse, since such large amounts of HCN require the hot, inner envelope to survive for over $10^4$ yr.

Another key difference between the two models concerns the distribution of sulfuretted molecules. In both models, the evaporated $H_2S$ is initially processed into a variety of S-bearing species, but in the collapse model a trace amount of $H_2S$ remains in the gas and CS and SO are the dominant species. In the static model, the chemistry has more time to evolve, more $H_2S$ is destroyed, and at late times SO is further oxidized to $SO_2$. Gas-phase $SO_2$ abundances of $\sim 10^{-7}$ have been observed toward a number of massive protostars by Keane et al. (2001). As with the HCN observations discussed above, this is further evidence that these envelopes must be supported against collapse, allowing sufficient time ($\sim 10^4$–$10^5$ yr) for warm postevaporation chemistry to produce the observed abundances. In hot cores $H_2S$ is removed

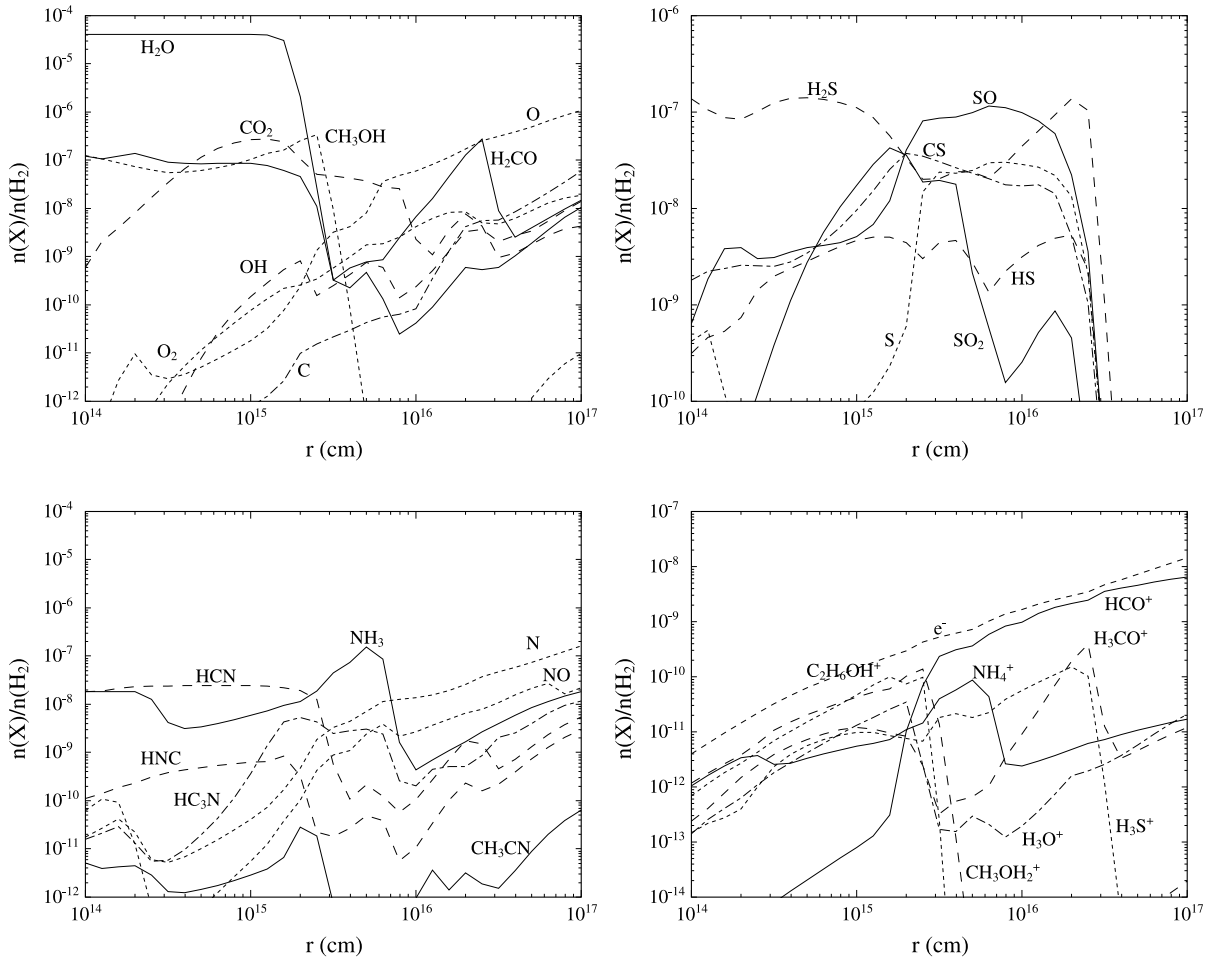


FIG. 5.—Molecular abundances in a static protostellar envelope, $10^4$ yr after the protostar "switches on" and begins to heat the gas

rapidly as it is destroyed by atomic H to give HS and S (Charnley 1997). However, at temperatures above 400 K, reverse reactions with $H_2$ become important, i.e.,

$$\mathrm{H_2S} \underset{\mathrm{H_2}}{\overset{\mathrm{H}}{\rightleftharpoons}} \mathrm{HS} \underset{\mathrm{H_2}}{\overset{\mathrm{H}}{\rightleftharpoons}} \mathrm{S}\,, \tag{11}$$

so $H_2S$ becomes the dominant species in the very inner envelope. The "spiky" nature of Figure 6 is partially due to the low spatial resolution—we have only 31 points along the radial axis—but is mostly due to the complex nature of the sulfur chemistry and the detailed time and temperature dependence of the abundances of sulfuretted molecules. At later times in this model, the CS emission solely traces the outer envelope.

## 5. DISCUSSION

### 5.1. *Binding Energies and Molecular Distributions*

Because the sublimation of molecular ices depends exponentially on the temperature, we find that the gas-phase abundances of parent species exhibit sharp jumps at particular radii, which depend on the surface binding energies, $E_b$, of the molecules. We find that these sublimation fronts are located at distances that scale as $E_b^{-2.5}$, and that they move outward with time as the protostellar luminosity increases. For the temperature distribution calculated by Adams & Shu (1985) we find that the radius is proportional to $t^{0.5}$ (eq. [10]).

The resulting spatial differentiation is most apparent in sulfuretted molecules because our assumed S-bearing parent, $H_2S$, has a lower binding energy than most other parent molecules (see § 4.1), which results in a large region of the envelope where $H_2S$ is the only gas phase parent molecule. Hence, maps of sulfuretted molecules in hot cores should reveal a much larger extent than O- and N-bearing species related to $H_2O$, $CH_3OH$, and $NH_3$. This result is, however, dependent on two crucial assumptions. First, we have assumed that $H_2S$ is the dominant form of sulfur in the ices. This is consistent with the observed fact that the major ice species are simple hydrides, with previous hot-core models that show that sublimation of $H_2S$ can explain the abundances of most other S-bearing molecules (Charnley 1997), and also with the fact that $H_2S$ appears to be the most abundant sulfuretted molecule in cometary ices (Bockelée-Morvan et al. 2000). Nevertheless, OCS is the only solid-state S-bearing molecule as yet detected in interstellar ices (Palumbo, Geballe, & Tielens 1997). If the principal reservoir of grain surface sulfur is some molecule less volatile than $H_2S$, the distribution of sulfuretted molecules in hot cores will be less extended than we calculate.

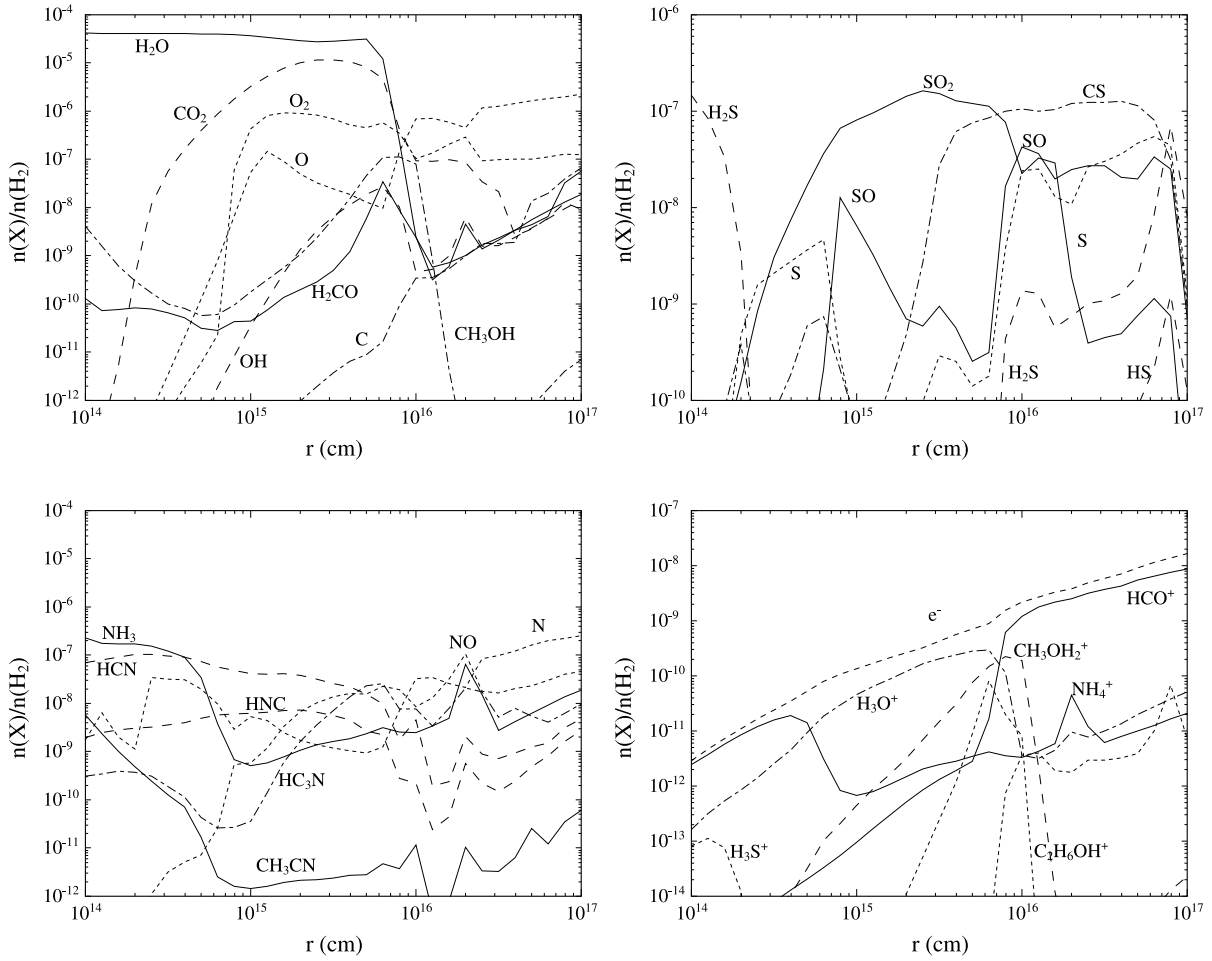


FIG. 6.—As Fig. 5, but $t = 10^5$ yr

Second, we use a value of 1800 K for the binding energy of $H_2S$ to grains (Aikawa et al. 1997). This is an estimate, rather than a laboratory measurement, so the true value may be higher. In addition, it is not clear that the appropriate value to use for the binding energy is that of the pure substance. Water is the dominant constituent of the polar component of interstellar ices. Thus, the binding energy of $H_2S$ will depend on the structure of the $H_2O$ ice matrix and the positions of the $H_2S$ molecules within it. Experimental work on the trapping and outgassing of minor species in water ice reveal a complex temperature dependence for the sublimation rate (e.g., Bar-Nun et al. 1985). Observations of comet Hale-Bopp did not show any evidence for significant excess $H_2S$ production at large heliocentric distances (Biver et al. 1997), suggesting that $H_2S$ in cometary ices is no more volatile than other parent species.

If these results are also applicable to interstellar ices, our calculations may have significantly overestimated the size of the region where $H_2S$ is released from grains. Despite this, it remains the case that the distance of the sublimation front depends on the binding energy, so mapping of molecular distributions in hot cores may be used to constrain the relative volatility of interstellar ice mantle constituents.

### 5.2. *Spatial Differentiation in Hot Cores*

One of the original motivations for this study was to explain the observed N/O differentiation seen in many hot cores (see § 1). We have previously demonstrated that such differentiation can arise as an age/temperature effect—an O-rich chemistry develops at early times in warm gas, whereas hotter gas eventually evolves into an N-rich state (Paper I). Because many nitrile species are observed to have very compact source sizes as compared with O-bearing species (Gibb et al. 2000a), this will occur naturally if the central regions of the hot core are older and hotter than the outer regions. Our earlier simple model was unable to translate the predicted age/temperature dependence into a spatial dependence. Figures 7 and 8 show the spatial distributions and temporal evolution for a number species in the collapse and static models, respectively.

If we take large HCN and $CH_3CN$ abundances to be indicative of "N-richness" and $CH_3OH$ and $(CH_3)_2O$ as measures of "O-richness," it is clear from Figure 7 that in collapsing cores these molecules tend to coexist. It is possible that chemical differentiation between different cores may be related to the age, since $(CH_3)_2O$ is most abundant at early times, whereas HCN and $CH_3CN$ form later on (cf. Paper I). However, as discussed in § 4.2, collapsing cores

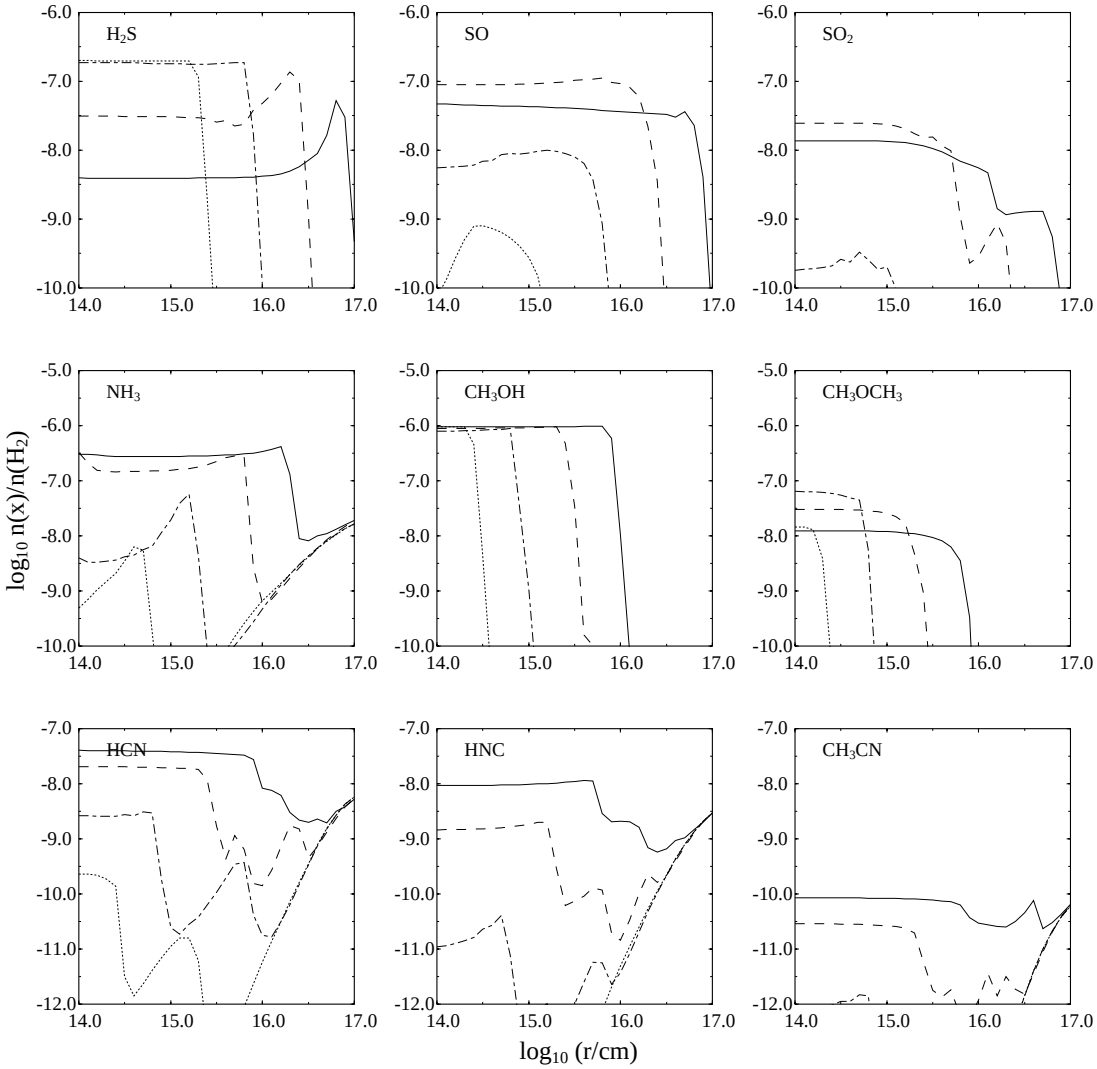


FIG. 7.—Spatial distributions of important molecules in a collapsing envelope. The results are plotted at times of $10^2$ (*dotted line*), $10^3$ (*dash-dotted line*), $10^4$ (*dashed line*), and $10^5$ (*solid line*) yr.

cannot account for small-scale structure within individual cores and cannot account for the large abundances of daughter molecules that are observed in many such objects. In static cores, on the other hand, much more complex spatial structures can develop (Fig. 8). For example, SO and $SO_2$ have central "holes" in their distributions, as do $CH_3OH$ and $(CH_3)_2O$ at late times. Thus, these species will tend to trace cooler gas than those that are concentrated in the hotter, inner, region. We find that high-temperature chemistry in the inner core leads to large amounts of HCN and $CH_3CN$, with the latter having a particularly sharp central peak in the static envelope. As discussed in § 4.2, because we have only small amounts of ammonia in the ices, both models produce similar HCN yields. In order to reproduce the observed HCN abundances, it is necessary to have both more initial $NH_3$ ice *and* to assume the core is not collapsing.

We have previously shown that if ammonia is present in the ices with a similar abundance to methanol, large abundances of O-rich molecules cannot be produced (Paper I). This is because $NH_3$ acts as a "proton sink" and thus destroys the $CH_3OH_2^+$ ions that form large O-bearing organics. If ammonia is indeed present in the ices at the $\sim$10% level, it is necessary to find some other way to explain the existence of O-rich, N-poor regions. One possibility is that methanol evaporates at lower temperatures than ammonia, leading to an extended region of the envelope where $CH_3OH$ is the predominant gas-phase species. This cannot be the case if the desorption is controlled by the binding energies of the pure substance, since $CH_3OH$ is less volatile than $NH_3$ (Sandford & Allamandola 1993). However, if methanol is present in amorphous $H_2O$ ice at more than the 7% level, the excess $CH_3OH$ may be expelled when the system crystallizes into a clathrate structure (Blake et al. 1991). If ammonia molecules remain trapped in the $H_2O$ ice, this could account for the presence of $CH_3OH$-rich, $NH_3$-poor regions. Dartois et al. (1999a) showed that much of the solid-state methanol toward protostars is in the form of a $CH_3OH$—$CO_2$ complex, which will alter the effective sublimation temperature of the $CH_3OH$. However, Ehrenfreund et al. (1998b) investigated the properties of interstellar ice analogs upon heating and demonstrated that $CH_3OH$, $H_2O$, and $CO_2$ form complexes that keep them from subliming until higher temperatures. Thus, it appears unlikely

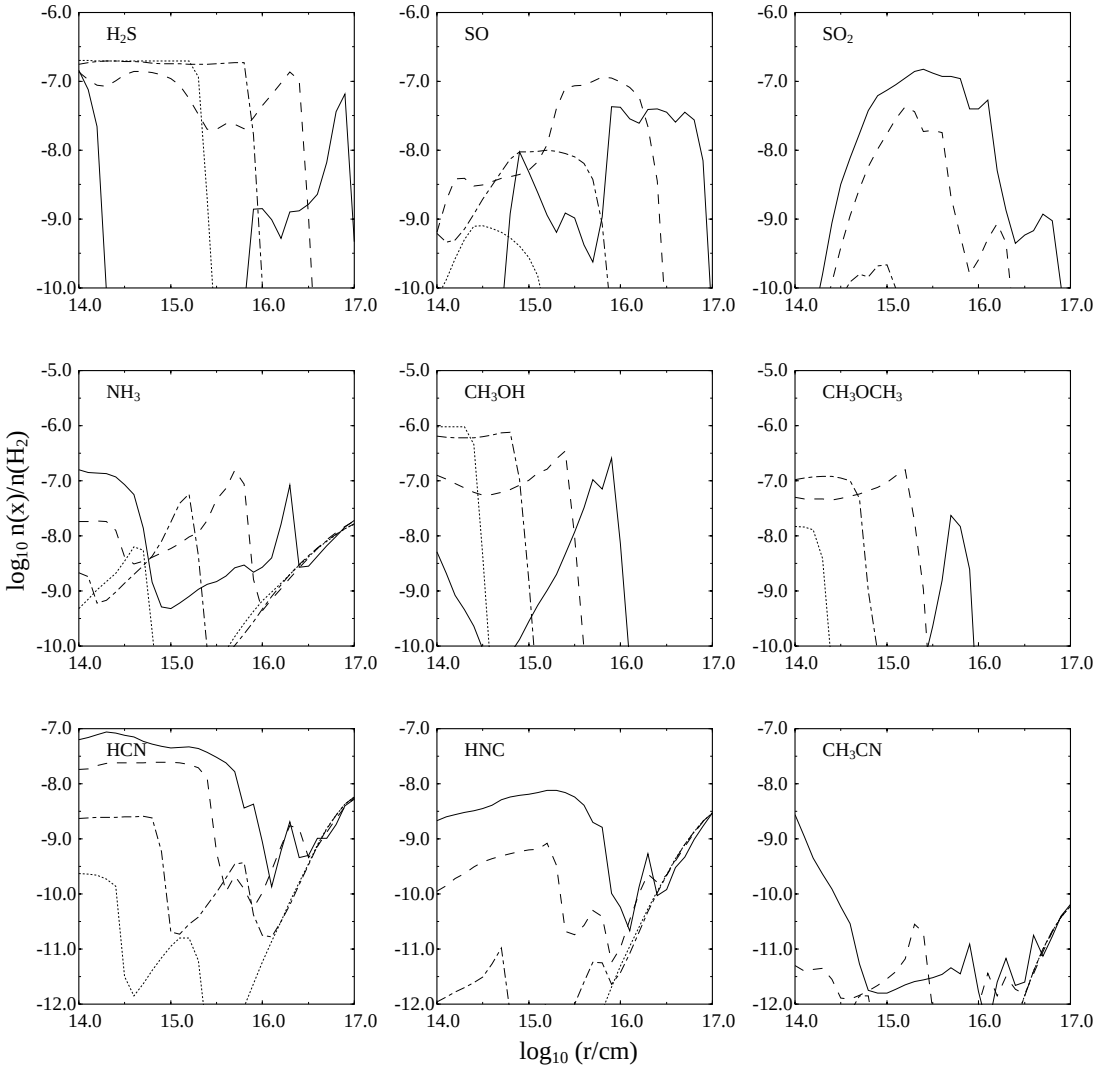


FIG. 8.—As Fig. 7, but for the static model

that significant $CH_3OH$ desorption can occur without $NH_3$ also having been released.

Alternatively, even if $CH_3OH$ and $NH_3$ are evaporated simultaneously, if the $CH_3OH$ abundance is large enough it may be able to overcome the competition from ammonia for protons, and sufficient $CH_3OH_2^+$ could be present to form O-rich cores. Huge abundances of solid-state methanol (~30%) have been seen toward two protostars by Dartois et al. (1999b); such large amounts may be related to energetic processing of ices, perhaps by cosmic rays (e.g., Hudson & Moore 1999).

Finally, recent observations of interstellar ices show that solid-state $NH_3$ has a fairly low abundance toward many sources (Dartois & d'Hendecourt 2001; Gibb et al. 2001). This appears to conflict with our conclusion that the observed level of HCN can be produced only if $NH_3$ is present in the evaporated ices. A possible explanation for this apparent discrepancy is that it is a result of a "selective depletion" phase of chemical evolution. Recent observations have demonstrated that the centers of prestellar cores are depleted in CO relative to $N_2$ (Bergin et al. 2002; Tafalla et al. 2002); the resulting chemical evolution of these cores can lead to large amounts of solid $NH_3$ and may result in a large fraction of the nitrogen being in atomic rather than molecular form (Charnley & Rodgers 2002). These regions subsequently become the innermost, hottest regions of the hot core, and the large $NH_3$ and $N^0$ abundances may account for the rapid formation of HCN and larger nitriles.

### 5.3. *Column Densities*

In order to compare our model with observations it is necessary to calculate column densities, obtained by integrating the number density along the path of the telescope beam, i.e., $N = \int n(r)dr$. For a homogeneous source this is clearly trivial, and $N = nL$, where $L$ is the linear size of the source. However, for a centrally peaked source the column densities will depend on whether the source is resolved by the telescope and the size of the telescope beam. In general, it is not possible to talk about a single, "true" value of $N$ in such sources, since the observed value depends on the telescope (see Nummelin et al. 2000 for a thorough discussion on the problems of translating column densities into molecular abundances). However, if one integrates along a very narrow trajectory through the core, it is possible to calculate the resulting "pencil-beam" column density; this will

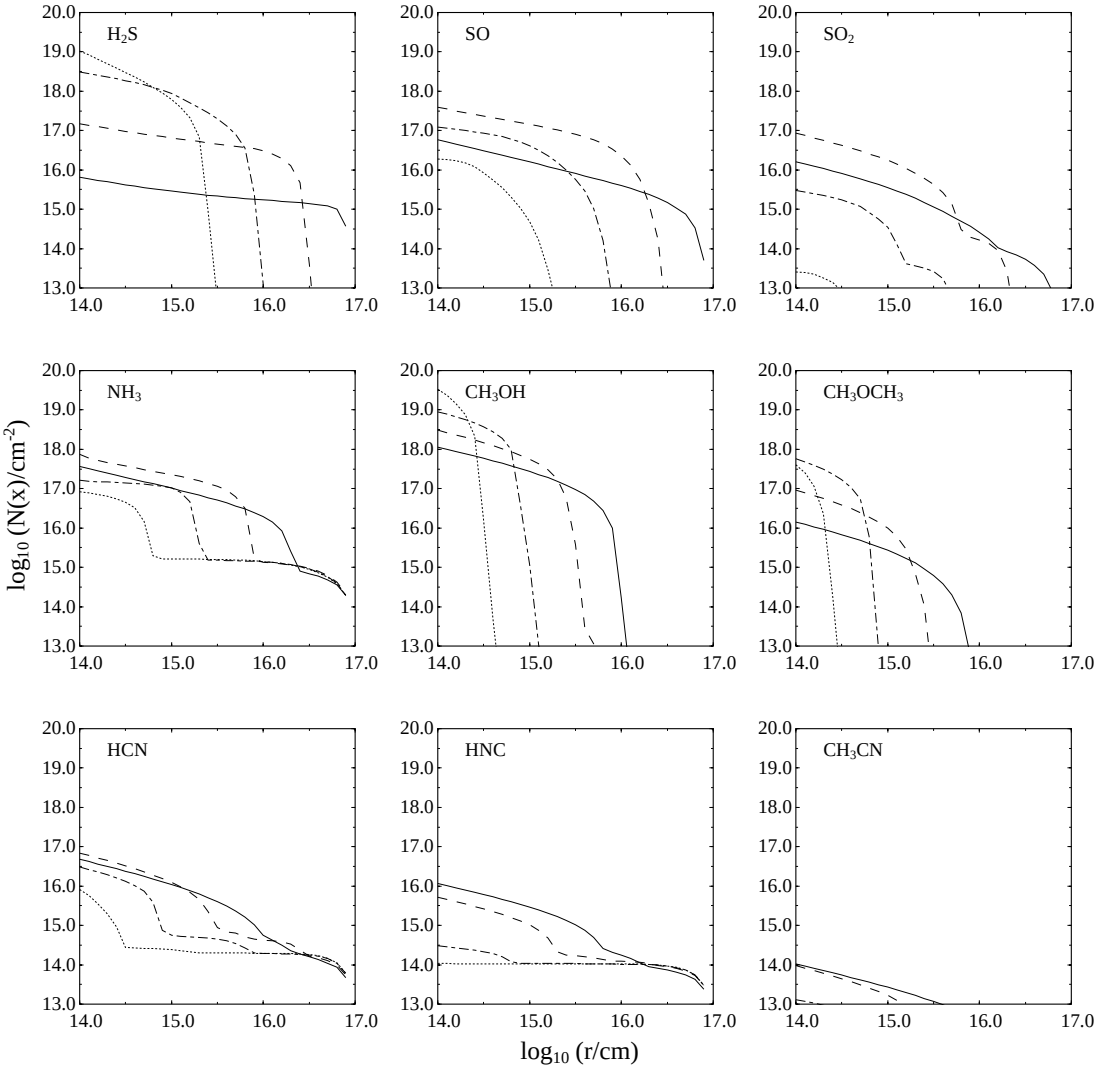


FIG. 9.—Pencil-beam column densities vs. offset from the core center for molecules in the collapsing envelope. As in Fig. 7, the results are plotted at times of $10^2$ (*dotted line*), $10^3$ (*dash-dotted line*), $10^4$ (*dashed line*), and $10^5$ (*solid line*) yr.

naturally depend on which trajectory one chooses, and so will depend on the offset distance from the center of the core. Figures 9 and 10 show the resulting values of $N$ versus offset for our collapse and static models, respectively. Note that, for parent species, the profiles in the inner region have the shape $N \propto r^{-1}$, as expected for an underlying $n \propto r^{-2}$ density distribution.

In principle, one can compare the results shown in Figures 9 and 10 with maps of the molecular distributions in hot cores. However, this is feasible only for the closest hot cores, since it requires a spatial resolution of $\lesssim 10^{16}$ cm. For comparison, at the distance of Sgr B2 this corresponds to less than 0″.1. Because of the large distances of most hot cores, they are almost always much smaller than the typical beam sizes appropriate for single-dish millimeter and submillimeter observations. In this case, we have the simplifying circumstance that the total number of molecules seen by the telescope is independent of the beam size, and so the beam-averaged column density is simply inversely proportional to the beam area. This is can be accounted for via the introduction of a "beam filling factor," which can be calculated either by assuming a fixed source size or in more sophisticated treatments from $\chi^2$-minimization fits to different line parameters (e.g., Nummelin et al. 2000). In order to allow a rough comparison with observations, we have calculated the column densities appropriate for a circular Gaussian beam with a FWHM of $2 \times 10^{16}$ cm. This is sufficient to resolve almost all the emission from prototypical hot-core molecules such as $CH_3OH$, $NH_3$, $H_2O$, and so on, since their gas-phase abundances are low outside this radius. Thus, the column density actually observed by a telescope with beam radius $b$ will be equal to this value multiplied by the beam dilution factor $(10^{16}\ \mathrm{cm}/b)^2$. Of course, this will not apply to those molecules that have an extended source much larger than the hot-core size.

Figure 11 shows the evolution of these "source-averaged" column densities with time. It is clear that much more HCN and $SO_2$ are formed at late times in the static envelope but that the column densities for other species are similar in both models. This illustrates the importance of interferometric mapping of hot cores, since large telescope

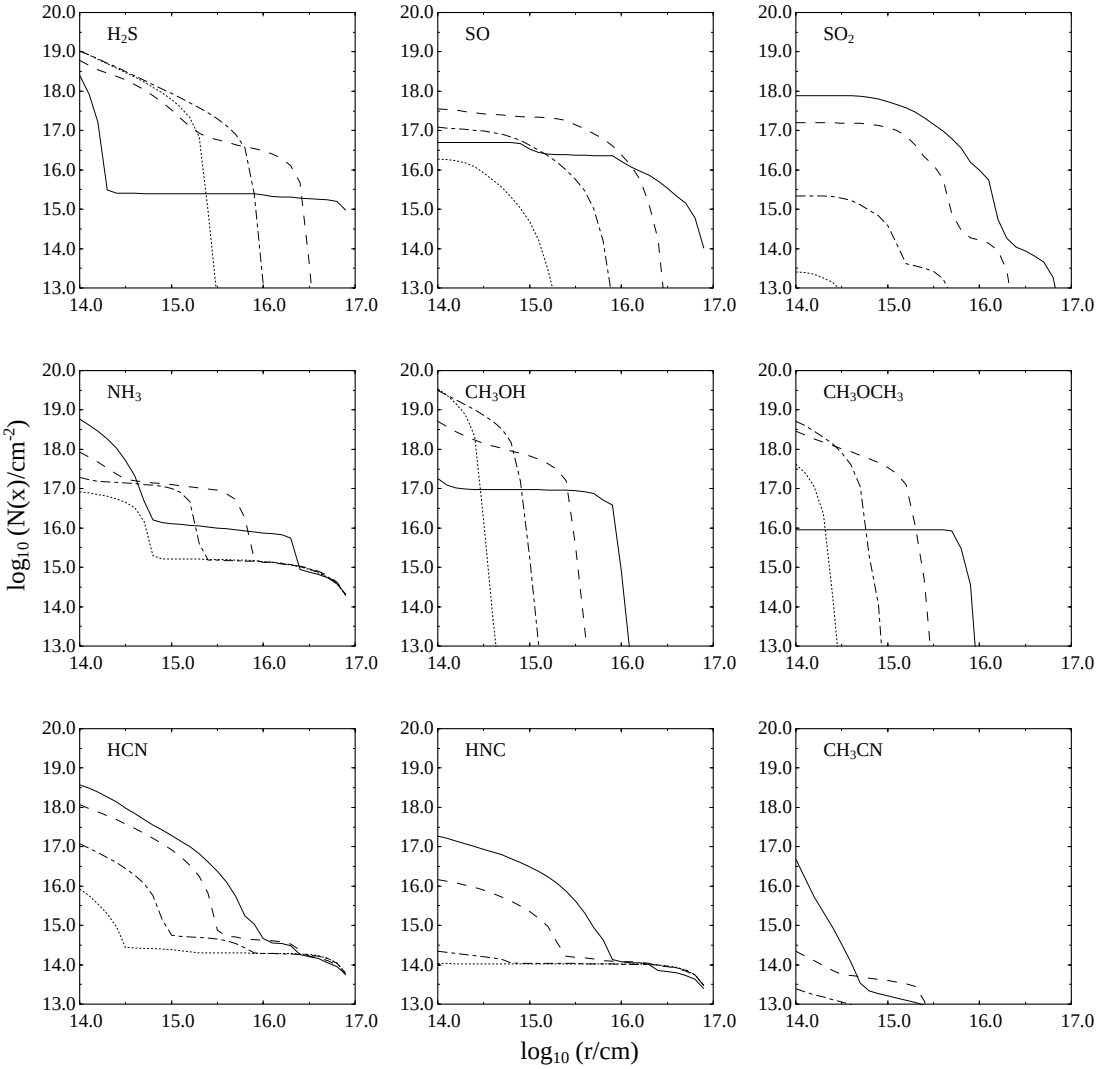


FIG. 10.—As Fig. 9, but for the static model

beams are unable to resolve any of the small-scale structure that may be present in the inner regions.

### 5.4. *The Link between Chemistry and Cloud Dynamics*

As discussed in § 3.1, neither of our models represents a fully realistic description of the physical conditions in actual protostellar envelopes. Nevertheless, our models describe the extremes of behavior likely to be found in protostellar cores; from outright gravitational free-fall collapse with virtually no support to a fully supported envelope that is not collapsing at all. Important differences in our model results can be used to identify key molecules whose abundance trace whether or not the cores are collapsing rapidly.

Our results show that in rapidly collapsing cores, only a limited amount of chemical processing can occur. This occurs because the gas is accelerating as it falls inward and so spends only a short time in the high-temperature region before it is incorporated into the growing protostar. Since the sublimation fronts have a radius proportional to $(t)^{1/2}$ (eq. [10]), whereas the collapse wave front has a radius equal to $at$, the collapse wave soon overtakes the sublimation fronts. For typical values of the sound speed, and for molecules with sublimation temperatures of $\approx$70–100 K, this occurs within 1000 yr. After this time, newly evaporated parent molecules are injected into gas that is already falling in toward the central protostar, and the dynamical timescale is much less than the chemical timescale of $\sim 10^4$ yr required to form significant abundances of daughter molecules. Hence, in the collapse model, small-scale structure due to temperature-dependent chemistry in the inner envelope cannot occur.

The wide variety of molecules seen in many hot cores are thought to result from postsublimation chemistry. As we have shown that such chemistry cannot occur in rapidly collapsing material, we therefore conclude that massive hot cores are supported. This is not to say that hot cores must be totally static; observations of line profiles suggest that the gas in some hot cores is indeed undergoing infall (Zhang, Ho, & Ohashi 1998), and it is possible that the colder gas in the outer envelope is collapsing onto the hot core (Maxia et al. 2001). However, the hot gas in the innermost regions must be able to survive for at least $10^4$ yr if the observed abundances are to be explained.

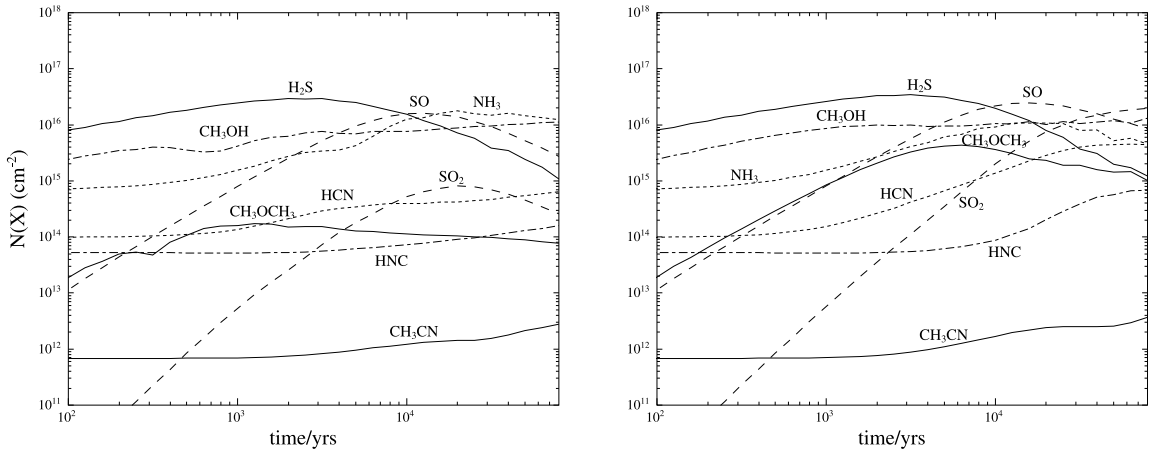


FIG. 11.—"Source-averaged" column densities vs. time for the species shown in Figs. 7–10. *Left*: Collapse model. *Right*: Static model. These column densities are calculated by convolving the results shown in Figs. 9 and 10 with a Gaussian telescope beam of FWHM $2 \times 10^{16}$ cm.

For low-mass hot cores, many fewer molecules have been studied, so it is hard to constrain their dynamical state from the chemistry. Low-mass protostellar envelopes undergoing inside-out collapse lead us to expect that low-mass hot cores should have simpler chemical compositions than their high-mass counterparts, consisting mainly of the sublimated parent species.

### 5.5. *Hot-Core Abundances and Grain Surface Chemistry*

Our conclusions reached in the previous section depend on the assumption that many of the molecules seen in hot cores are daughter species, formed in situ in the hot gas. Alternatively, it could be the case that the observed complexity results from grain surface chemistry (e.g., Caselli et al. 1993). However, it is very difficult to explain the observed chemical composition in hot cores with a general surface chemical model. If one places reasonable constraints on the type of reactions that can occur on grain surfaces, some degree of postsublimation gas phase chemistry appears to be essential (Charnley 2001). Also, the large HCN abundance of $10^{-6}$ observed toward the protostar GL 2591 cannot be explained simply by sublimation but requires HCN to be synthesized in high-temperature reactions (Boonman et al. 2001). This is consistent with *Infrared Space Observatory* observations, which place an upper limit to solid-state HCN of 3% relative to $H_2O$ (Gibb et al. 2000b), implying a postsublimation gas-phase HCN abundance of $\lesssim 3 \times 10^{-7}$. A similar problem arises for larger nitrile species; summing the observed abundances in the hot core G327.3−0.6 and converting to a solid-state optical depth should result in a broad absorption feature at 4.3–4.6 $\mu$m, which is not seen (Gibb et al. 2000a). Therefore, it appears that the observed nitriles must be formed in the gas phase.

## 6. CONCLUSION

Hot molecular cores develop when protostars heat their natal cocoons of gas and dust and icy grain mantles are released into the gas phase. Previous models of hot cores have focused on the chemical evolution and have made many simplistic assumptions regarding the physical conditions. Some models have considered spatial density variations and gradual heating of the gas, we have combined these approaches, using physically realistic values for $n$ and $T$ obtained from models of protostellar collapse and envelope heating. Below, we summarize our major results:

1. As the growing protostar heats the surrounding gas, sublimation fronts travel outward through the protostellar envelope. The distances of these fronts from the central star depend on the sublimation temperature of each species, and for the temperature distribution calculated by Adams & Shu (1985) we find that they increase with time as $t^{0.5}$.

2. The distance of the sublimation front depends on the binding energy of each species, and we find, as expected, that hot cores should display an onion-skin type structure, with more volatile molecules being released at larger distances. Thus, mapping of hot cores may be used to infer the relative sublimation temperatures of different interstellar ice constituents. This effect is particularly pronounced for the sulfur chemistry, due to the low binding energy of $H_2S$, which we have assumed to be the principal sulfuretted molecule in the ices.

3. Important chemical differences are evident between models that assume that the core is undergoing collapse and models that assume a static envelope. In the first case, as the infalling gas accelerates, the dynamical timescale in the inner envelope becomes less than the chemical timescale, and we find that the abundances in the inner core are the same as those set in the outer regions. In our static model the hot gas survives for much longer and significant chemical processing can occur. Because many of the molecules observed in massive hot cores are thought to be daughter molecules, this implies that the gas in these cores must be supported against collapse over timescales of at least $10^4$ yr.

4. In the static model, small-scale spatial structure is evident in the molecular abundances in the inner regions. This may account for the observed O-rich versus N-rich segregation that is evident in many hot cores, since the inner regions are hotter and older (in terms of the time since the ices evaporated), and older, hotter gas tends to evolve toward an N-rich state (Paper I).

5. In order to prevent the surrounding envelope from collapsing for the required timescales of $\sim 10^4$ yr, the core must have a source of support. Such a situation is most

viable for massive protostars. Hence, low-mass hot cores are more likely to exhibit a simpler chemistry than massive hot cores.

In order to compare the abundances of our models, it is important to obtain high-resolution maps of molecular distributions in hot cores. To date, high-mass cores have been studied in much greater detail than low-mass cores. More observations of low-mass protostellar envelopes are required in order that systematic comparisons can be made between the two. Also, because the sublimation of molecules depends sensitively on the surface binding energy, laboratory measurements of the desorption rates of realistic interstellar ice analogs are essential. Finally, it is also possible that at least some hot cores result from shocks (Charnley & Kaufman 2000). Future theoretical work should focus on identifying other chemical tracers of shocked gas (Viti et al. 2001).

Theoretical astrochemistry at NASA Ames is supported by NASA's Origins of Solar Systems, LTSA, and Exobiology Programs through NASA Ames Interchange NCC2-1162. S. D. R. was initially supported by a National Research Council postdoctoral research associateship (Viti et al. 2001).

## REFERENCES

Adams, F. C., & Shu F. H. 1985, ApJ, 296, 655
Aikawa, Y., Herbst, E., & Dzegilenko, F. N. 1999, ApJ, 527, 262
Aikawa, Y., Ohashi, N., Inutsuka, S.-I., Herbst, E., & Takakuwa, S. 2001, ApJ, 552, 639
Aikawa, Y., Umebayashi, T., Nakano, T., & Miyama, S. M. 1997, ApJ, 486, L51
André, P., Ward-Thompson, D., & Barsony, M. 2000, in Protostars and Planets IV, ed. V. Mannings, A. P. Boss, & S. S. Russell (Tucson: Univ. Arizona Press), 59
Bar-Nun, A., Herman, G., Laufer, D., & Rappaport, M. L. 1985, Icarus, 63, 317
Bergin, E. A., Alves, J., Huard, T., & Lada, C. J. 2002, ApJ, 570, L101
Bergin, E. A., & Langer, W. D. 1997, ApJ, 486, 316
Biver, N., et al. 1997, Earth, Moon, & Planets, 78, 5
Blake, D., Allamandola, L. J., Sandford, S., Hudgins, D., & Freund, F. 1991, Science, 254, 548
Blake, G. A., Sutton, E. C., Masson, C. R., & Phillips, T. G. 1987, ApJ, 315, 621
Bockelée-Morvan, D., et al. 2000, A&A, 353, 1101
Boogert, A. C. A., Tielens, A. G. G. M., Ceccarelli, C., Boonman, A. M. S., van Dishoeck, E. F., Keane, J. V., Whittet, D. C. B., & de Graauw, Th. 2000, A&A, 360, 683
Boonman, A. M. S., Stark, R., van der Tak, F. F. S., van Dishoeck, E. F., van der Wal, P. B., Schäfer, F., de Lange, G., & Laauwen, W. M. 2001, ApJ, 553, L63
Brown, P. D., Charnley, S. B., & Millar, T. J. 1988, MNRAS, 231, 409
Caselli, P., Hasegawa, T. I., & Herbst, E. 1993, ApJ, 408, 548
Caselli, P., Walmsley, C. M., Tafalla, M., Dore, L., & Myers, P. C. 1999, ApJ, 523, L165
Ceccarelli, C., Castets, A., Caux, E., Hollenbach, D., Loinard, L., Molinari, S., & Tielens, A. G. G. M. 2000, A&A, 355, 1129
Ceccarelli, C., Hollenbach, D. J., & Tielens, A. G. G. M. 1996, ApJ, 471, 400
Ceccarelli, C., Loinard, L., Castets, A., Tielens, A. G. G. M., Caux, E., Lefloch, B., & Vastel, C. 2001, A&A, 372, 998
Charnley, S. B. 1997, ApJ, 481, 396
———. 2001, in Building Bridges from the Big Bang to Biology, Special Volume, ed. F. Giovannelli (Rome: Consiglio Nazionale delle Ricerche President Bureau), 139
Charnley, S. B., & Kaufman, M. J. 2000, ApJ, 529, L111
Charnley, S. B., Kress, M. E., Tielens, A. G. G. M., & Millar T. J. 1995, ApJ, 448, 232
Charnley, S. B., & Rodgers, S. D. 2002, ApJ, 569, L133
Charnley, S. B., Rodgers, S. D., & Ehrenfreund, P. 2001, A&A, 378, 1024
Charnley, S. B., Tielens, A. G. G. M., & Millar, T. J. 1992, ApJ, 399, L71
Dartois, E., & d'Hendecourt, L. 2001, A&A, 365, 144
Dartois, E., Demyk, K., d'Hendecourt, L., & Ehrenfreund, P. 1999a, A&A, 351, 1066
Dartois, E., Gerin, M., & d'Hendecourt, L. 2000, A&A, 361, 1095
Dartois, E., Schutte, W., Geballe, T. R., Demyk, K., Ehrenfreund, P., & d'Hendecourt, L. 1999b, A&A, 342, L32
Doty, S. D., & Neufeld, D. A. 1997, ApJ, 489, 122
Ehrenfreund, P., Boogert, A., Gerakines, P., & Tielens, A. G. G. M. 1998a, Faraday Discuss., 109, 463
Ehrenfreund, P., & Charnley, S. B. 2000, ARA&A, 38, 427
Ehrenfreund, P., Dartois, E., Demyk, K., & d'Hendecourt, L. 1998b, A&A, 339, L17
El-Nawawy, M. S., Howe, D. A., & Millar, T. J. 1997, MNRAS, 292, 481
Gibb, E., Nummelin, A., Irvine, W. M., Whittet, D. C. B., & Bergman, P. 2000a, ApJ, 545, 309
Gibb, E. L., Whittett, D. C. B., & Chiar, J. E. 2001, ApJ, 558, 702
Gibb, E. L., et al. 2000b, ApJ, 536, 347
Hatchell, J., Fuller, G. A., Millar, T. J., Thompson, M. A., & Macdonald, G. H. 2000, A&A, 357, 637
Hatchell, J., Thompson, M. A., Millar, T. J., & Macdonald, G. H. 1998a, A&A, 338, 713
———. 1998b, A&AS, 133, 29
Hudson, R. L., & Moore, M. H. 1999, Icarus, 140, 451
Kahn, F. D. 1974, A&A, 37, 149
Kaufman, M. J., Hollenbach, D. J., & Tielens, A. G. G. M. 1998, ApJ, 497, 276
Keane, J. V., Boonman, A. M. S., Tielens, A. G. G. M., & van Dishoeck, E. F. 2001, A&A, 376, L5
Kurtz, S., Cesaroni, R., Churchwell, E., Hofner, P., & Walmsley, M. 2000, in Protostars and Planets IV, ed. V. Mannings, A. P. Boss, & S. S. Russell (Tucson: Univ. Arizona Press), 299
Lahuis, F., & van Dishoeck, E. F. 2000, A&A, 355, 699
Larson, R. B. 1969, MNRAS, 145, 271
Loinard, L., Castets, A., Ceccarelli, C., Caux, E., & Tielens, A. G. G. M. 2001, ApJ, 552, L163
Markwick, A. J., Millar, T. J., & Charnley, S. B. 2000, ApJ, 535, 256
Maxia, C., Testi, L., Cesaroni, R., & Walmsley, C. M. 2001, A&A, 371, 287
McLaughlin, D. E., & Pudritz, R. E. 1997, ApJ, 476, 750
Millar, T. J., Farquhar, P. R. A., & Willacy, K. 1997a, A&AS, 121, 139
Millar, T. J., Herbst, E., & Charnley, S. B. 1991, ApJ, 369, 147
Millar, T. J., Macdonald, G. H., & Gibb, A. G. 1997b, A&A, 325, 1163
Mouschovias, T. 1978, in Protostars and Planets, ed. T Gehrels (Tucson: Univ. Arizona Press), 209
Nummelin, A., Bergman, P., Hjalmarson, Å., Friberg, P., Irvine, W. M., Millar, T. J., Ohishi, M., & Saito, S. 2000, ApJS, 128, 213
Osorio, M., Lizano, S., & D'Alessio, P. 1999, ApJ, 525, 808
Palumbo, M. E., Geballe, T. R., & Tielens, A. G. G. M. 1997, ApJ, 479, 839
Penston, M. V. 1969, MNRAS, 144, 425
Pratap, P., Megeath, S. T., & Bergin, E. A. 1999, ApJ, 517, 799
Rawlings, J. M. C., Hartquist, T. W., Menten, K. M., & Williams, D. A. 1992, MNRAS, 255, 471
Richer, J., Shepherd, D., Cabrit, S., Bachiller, R., & Churchwell, E. 2000, in Protostars and Planets IV, ed. V. Mannings, A. P. Boss, & S. S. Russell (Tucson: Univ. Arizona Press), 867
Rodgers, S. D., & Charnley, S. B. 2001a, ApJ, 546, 324 (Paper I)
———. 2001b, MNRAS, 320, L61
Rodgers, S. D., & Millar, T. J. 1996, MNRAS, 280, 1046
Sandford, S. A., & Allamandola, L. J. 1993, ApJ, 417, 815
Shu, F. H. 1977, ApJ, 214, 488
Spitzer, L. J. 1978, Physical Processes in the Interstellar Medium (New York: Wiley)
Stahler, S. W., Palla, F., & Ho, P. T. P. 2000, in Protostars and Planets IV, ed. V. Mannings, A. P. Boss, & S. S. Russell (Tucson: Univ. Arizona Press), 327
Stahler, S. W., Shu, F. H., & Taam, R. E. 1980, ApJ, 241, 637
Talbi, D., & Herbst, E. 1998, A&A, 333, 1007
Tafalla, M., Myers, P. C., Caselli, P., Walmsley, C. M., & Comito, C. 2002, ApJ, 569, 815
Thompson, M. A., & Macdonald, G. H. 1999, A&AS, 135, 531
Tielens, A. G. G. M., Tokunaga, A. T., Geballe, T. R., & Baas, F. 1991, ApJ, 381, 181
Umebayashi, T., & Nakano, T. 1990, MNRAS, 243, 103
van der Tak, F. F. S., van Dishoeck, E. F., & Caselli, P. 2000b, A&A, 361, 327
van der Tak, F. F. S., van Dishoeck, E. F., Evans, N. J., II, Bakker, E. J., & Blake, G. A. 1999, ApJ, 522, 991
van der Tak, F. F. S., van Dishoeck, E. F., Evans, N. J., II, & Blake, G. A. 2000a, ApJ, 537, 283
van Dishoeck, E. F., & Blake, G. A. 1998, ARA&A, 36, 317
van Dishoeck, E. F., Blake, G. A., Jansen, D. J., & Groesbeck, T. D. 1995, ApJ, 447, 760

Viti, S., Caselli, P., Hartquist, T. W., & Williams, D. A. 2001, A&A, 370, 1017
Viti, S., & Williams, D. A. 1999, MNRAS, 305, 755
Walmsley, C. M., & Schilke, P. 1993, in Dust and Chemistry in Astronomy, ed. T. J. Millar & D. A. Wiliams (Bristol: IOP), 37
Watson, W. D., & Salpeter, E. E. 1972, ApJ, 174, 321
Willacy, K., & Millar., T. J. 1998, MNRAS, 298, 562
Wilson, T. L., Gaume, R. A., Gensheimer, P., & Johnston, K. J. 2000, ApJ, 538, 665
Wyrowski, F., Schilke, P., Walmsley, C. M., & Menten, K. M. 1999, ApJ, 514, L43
Yorke, H. W., & Krügel, E. 1977, A&A, 54, 183
Zhang, Q., Ho, P. T. P., & Ohashi, N. 1998, ApJ, 494, 636